Journal of Magnetism and Magnetic Materials 427 (2017) 345–351

Contents lists available at ScienceDirect

Journal of Magnetism and Magnetic Materials

journal homepage: www.elsevier.com/locate/jmmm

Development of a real time imaging-based guidance system of magnetic nanoparticles for targeted drug delivery

Xingming Zhang[a,b], Tuan-Anh Le[b], Jungwon Yoon[b,*]

[a] School of Naval Architecture and Ocean Engineering, Harbin Institute of Technology at Weihai, Weihai, Shandong, China
[b] School of Mechanical and Aerospace Engineering & ReCAPT, Gyeongsang National University, Jinju 660-701, Republic of Korea

ARTICLE INFO

Keywords:
Magnetic particle imaging
Nanoparticles
Electromagnetic actuator
Guidance system
Targeted drug delivery

ABSTRACT

Targeted drug delivery using magnetic nanoparticles is an efficient technique as molecules can be directed toward specific tissues inside a human body. For the first time, we implemented a real-time imaging-based guidance system of nanoparticles using untethered electro-magnetic devices for simultaneous guiding and tracking. In this paper a low-amplitude-excitation-field magnetic particle imaging (MPI) is introduced. Based on this imaging technology, a hybrid system comprised of an electromagnetic actuator and MPI was used to navigate nanoparticles in a non-invasive way. The real-time low-amplitude-excitation-field MPI and electro-magnetic actuator of this navigation system are achieved by applying a time-division multiplexing scheme to the coil topology. A one dimensional nanoparticle navigation system was built to demonstrate the feasibility of the proposed approach and it could achieve a 2 Hz navigation update rate with the field gradient of 3.5 T/m during the imaging mode and 8.75 T/m during the actuation mode. Particles with both 90 nm and 5 nm diameters could be successfully manipulated and monitored in a tube through the proposed system, which can significantly enhance targeting efficiency and allow precise analysis in a real drug delivery.

1. Introduction

In biological interactions, magnetic nanoparticles can function at both the cellular and molecular level [1], making them suitable for use as contrast agents in magnetic particle imaging (MPI) [2] and as carriers for targeted drug delivery. In the first human trials of this drug targeting technique, drugs were attached to 100 nm diameter iron-core particles and then concentrated by an external magnet field to treat tumors [3]. Our previous work demonstrated the delivery of 770 nm magnetic particles using an electromagnetic actuator into the brains of mice based on an open-loop control approach using extensive simulations [4,13]. These magnetic nanoparticles contain a fluorophore and have been engineered to enable tracking of their locations even after introduction in the body through blood. However, a guidance system capable of performing both actuation and monitoring of nanoparticles would be extremely useful to precisely steer the nanoparticles and track the nanoparticles in real-time through a feedback control. Several methods have been suggested to develop the targeting scheme with feedback control such as using an ultrasound for the locations of solid micro-size particles [5], or using microscope to track the visible particles [6]. Magnetic resonance navigation is the most efficient method for feedback control of targeted drug delivery. Magnetic resonance navigation is mainly based on magnetic nanoparticles embedded in micro carriers, which are controlled and tracked by Magnetic Resonance Imaging systems [7,8]. However, the major challenges faced in a targeting system are generating high gradient fields to steer the nanoparticles and tracking nanoparticles in real-time to enable precise targeting [9].

Magnetic Particle Imaging is a new tracer imaging modality that is gaining significant interest from Nuclear Magnetic Resonance Imaging researchers [10]. MPI scanners can achieve fast and high-sensitivity with millimeter-scale resolutions, and it has high potentials to revolutionize the biomedical imaging field. Tracer nanoparticles in MPI can provide the spatial information and it can be used as drug carrier particles. In MPI, the detection threshold of magnetic tracers is less limited by background signal from the host tissue compared to Magnetic Resonance Imaging [11]. Currently, an alternating field with a frequency of 25 kHz, amplitude of 20 mT/μ_0 is widely used in MPI [2].

For a brain specific targeting to cross blood brain barriers and nanoparticles' imaging inside a body, we have developed a MPI-based real time navigation system that simultaneously actuates and monitors magnetic nanoparticles in a noninvasive way. The proposed imaging method features an excitation field in a high frequency of 40 kHz and

* Corresponding author.
E-mail address: jwyoon@gnu.ac.kr (J. Yoon).

http://dx.doi.org/10.1016/j.jmmm.2016.10.056
Received 27 June 2016; Received in revised form 1 October 2016; Accepted 11 October 2016
Available online 13 October 2016
0304-8853/

low amplitude of 0.2 mT/μ_0, which is safe for medication due to the reduction of probability of unpleasant peripheral nerve stimulation [12]. Based on this imaging concept and our electromagnetic actuator [13], a one-dimensional navigation system for a mouse-size has been built and validated with both 90 nm and 5 nm particles, respectively. The results suggests that the MPI-based navigation system is capable of controlling the nanoparticles in real-time with a closed-loop control scheme.

2. MPI-based real time navigation system

2.1. Actuator of navigation system

To steer the magnetic particles in a noninvasive way, it is necessary to use a magnetic field gradient. Electromagnetic actuation systems [13] can induce a three-dimensional (3D) directional magnetic force, which is proportional to the amplitude of the gradient vector according to:

$$\mathbf{F}_m = V_{SPIO}(\mathbf{M}\cdot\nabla)\mathbf{B} \tag{1}$$

where $\mathbf{B}$ is the magnetic field vector, V_{SPIO} is the volume of the super paramagnetic iron oxide (SPIO) component of a single nanoparticle and $\mathbf{M}$ is the magnetization length of the nanoparticles. The 3D directional magnetic field is generated by three pairs of differential-current coils (DCC), with each pair guiding the magnetic particles in a particular direction. DCC arrangement [13] combines the properties of Helmholtz and Maxwell coils configurations in one set of coils. For a drug to be able to cross the blood-brain barrier or to be steered to a desired direction at a vascular bifurcation, the magnetic propulsion force should overcome the drag force:

$$\mathbf{F}_d = -3\pi\eta d_p(\mathbf{v}_p - \mathbf{v}) \tag{2}$$

where d_p is the particle diameter, η is the dynamic viscosity of blood, v is the velocity of the fluids, and v_p is the particle velocity.

2.2. The low amplitude excitation field MPI

Magnetic particle imaging (MPI) is an imaging technique based on the nonlinear magnetization characteristics of superparamagnetic iron oxide (SPIO) nanoparticles. When a high-frequency excitation field is applied to the nanoparticles, they respond by inducing a voltage signal in the receive coil. For spatial encoding, a gradient magnetic field called the selection field is applied. The purpose of the selection field is to obtain a point where the magnetic field is zero, called the field free point (FFP). A drive field is required to move the FFP in field of view. The trajectory of the FFP in the field of view depends on the current signal's amplitude and frequency in the drive field coils. By applying the excitation field, the particles induce sine signals with different amplitudes as shown in Fig. 1. If the particles are exposed to the selection field and an excitation magnetic field with amplitude smaller than the saturation field of magnetic nanoparticles is applied, oscillating.

magnetization will occur only at the particles of FFPs. The magnetic material located at the FFP only responds to the excitation field by an alternating current (AC). By controlling the trajectories of FFP over field of view and monitoring the particle magnetization responses, the particles concentration can be mapped to an image. The FFP can be moved in 3D using three orthogonal homogenous magnetic fields by three drive coil groups. In some researches, the oscillating magnetization and FFP movements can be realized by one coil group with high frequency and amplitude [2].

In the proposed low-amplitude-excitation-field MPI scheme, we use a drive field with a low frequency to move the FFP, while an excitation field with low amplitude and high frequency is used to achieve oscillating magnetization. But, the excitation field also induces the signals from a receiving coil, which do not have particles information. Thus, the cancellation coil is used to reduce the empty coil signal [14]. We can measure the concentration of particles in FFP from the amplitude of received signal by applying the amplitude modulation of the excitation field. Because a precise single excitation frequency is important, a band pass filter can diminish the harmonic interference induced by a power unit of excitation field. The signal detection and processing procedure for the low-amplitude-excitation-field MPI is shown in Fig. 2. Then, the MPI image can be acquired in real-time by the X-space reconstruction method [15]:

$$\mathrm{IMG}(x_s(t)) = \frac{s(t)}{B_1 mkG\dot{x}_s(t)} \tag{3}$$

where $x_s(t)$ is the position of FFP, $\dot{x}_s(t)$ is the speed of FFP, B_1 is the sensitivity of the receive coil, m is the magnetic moment of the magnetic nanoparticles, k is a property of the particle, G is the magnetic field gradient at FFP, and $s(t)$ is the signal induced by the nanoparticles. In the low-amplitude-excitation-field MPI, $s(t)$ can be replaced by $AMP(s(t))$ since the amplitude of the received signal indicates the concentration of nanoparticles. Then, the image reconstruction can be obtained as:

$$\mathrm{IMG}(x_s(t)) = \frac{\mathrm{AMP}(s(t))}{B_1 mkG\dot{x}_s(t)} \tag{4}$$

2.3. Navigation system and the control software

The coil topology of the 3D magnetic nanoparticle imaging-based navigation system is shown in Fig. 3. The 3D navigation system consists of three sets of actuation coils in a DCC arrangement, which enables us to steer the particles in 3D within the actuation period [13]. During the imaging period, one set of actuation coils (shown as z-direction in Fig. 3.) can be used as a selection field generator as well as a drive coil. The other two actuation coils sets were used as drive coils. Therefore, these three sets of actuation coils can make FFP pass through 3D field of view, called workspace, in a predetermined path. An excitation-generating coil and a signal- receiving coil around the workspace were used for generating oscillating fields with the excitation frequency and receiving signals from the particles, respectively. The experimental setup of the 1D nanoparticle navigation system, shown in Fig. 4., was devised to verify this design. The FFP can be created by two DCCs with opposite current direction. If sinusoidal

currents are coupled into the DCCs, the FFP will move inside the workspace [2]. The two actuation coils are powered by two power supplies, and sinusoidal signal generated by a functional generator is amplified by a power amplifier and the current fed to the excitation coil. The hardware connections for the proposed navigation system are shown in Fig. 5.

2.4. Integration of the navigation system

It is necessary to integrate the actuation module and the imaging module to implement a navigation system of nanoparticles. In this subsection, the time division, multiplexing scheme based on the LabVIEW software, which can control time sequencing, was proposed to integrate the electromagnetic actuator and MPI tasks. Every navigation period consists of at least one imaging scanning period to detect nanoparticles positions and one actuation period to control nanoparticles motions. During the actuation mode, magnetic fields will be high enough to saturate all the nanoparticles. The particles must be demagnetized before the imaging mode begins. Also, due to high impedance of DCCs, the currents in DCCs cannot be changed immediately between actuation and imaging mode. So, a relaxation period is introduced for demagnetizing time of particles and prevention of a voltage surge.

Since a relaxation period is required after each interval of actuation

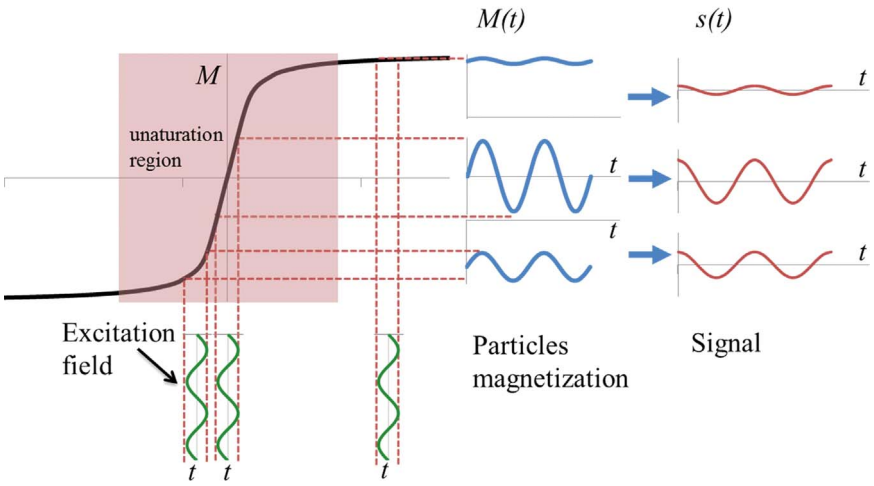

Fig. 1. The relation between an excitation field and the magnetization of a magnetic particle. During low amplitude of excitation field, the particles will be unsaturated. Then, a sinusoidal excitation (the green curves) field within the unsaturation field of particles will result in sinusoidal magnetization change with a different amplitude (the blue curves). These particles magnetization will generate the signals *s(t)* in sinusoidal waves (the red curves).

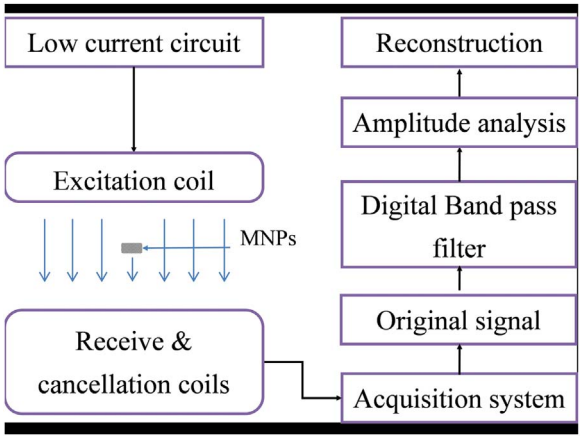

Fig. 2. Signal flow diagram of the realized setup.

and imaging mode, the hybrid time T_{hyb} in a period of navigation can be expressed as:

$$T_{hyb} = T_{mpi} + T_{ema} + 2T_{rel} \tag{5}$$

where T_{mpi}, T_{ema}, and T_{rel} are the MPI scanning time, the electromagnetic actuation time, and the relaxation time in a navigation period, respectively. A time division multiplexing scheme [16] can ensure the hybrid functionality of the navigation system and the navigation current I is given by:

$$I = ema(t)I_{ema} + mpi(t)I_{mpi} \tag{6}$$

where I_{ema} is the current to generate the guidance force of nanoparticles. I_{mpi} is the current to generate a selection field for movement of FFP in MPI, *ema(t)* and *mpi(t)* are the time sequences for electromagnetic actuation and MPI imagining cycles, respectively. Assume that every hybrid cycles begins with MPI mode, then the time sequences can be defined as:

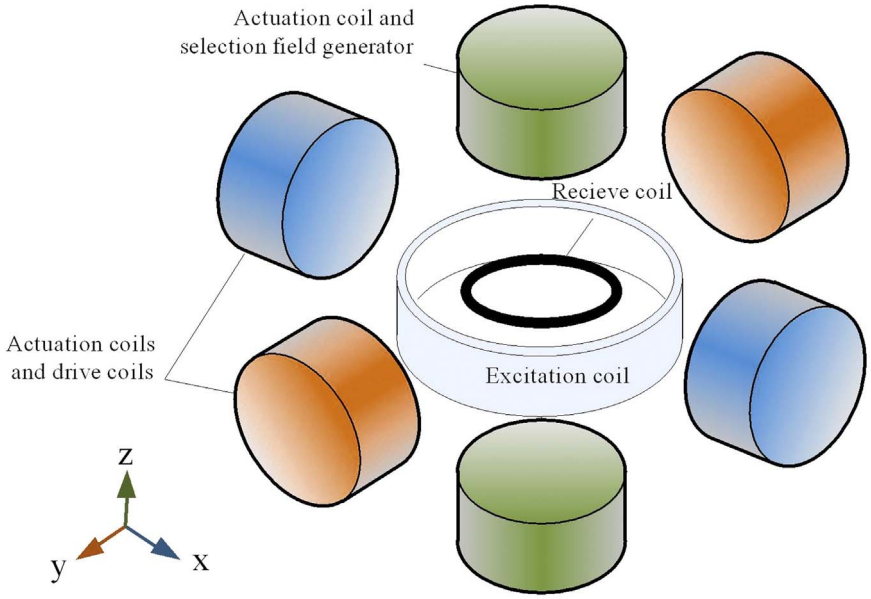

Fig. 3. Schematic diagram of the field-generating components of the magnetic nanoparticle navigation system. Two selection field generators induce and move a field free point. For each direction in space, two opposing drive coils are used to move the field free point. During imaging and actuation periods these coils induce a field gradient, which controls the nanoparticle. The excitation coil generates a field that controls the magnetization of the nanoparticles and the signal received by the receive coil.

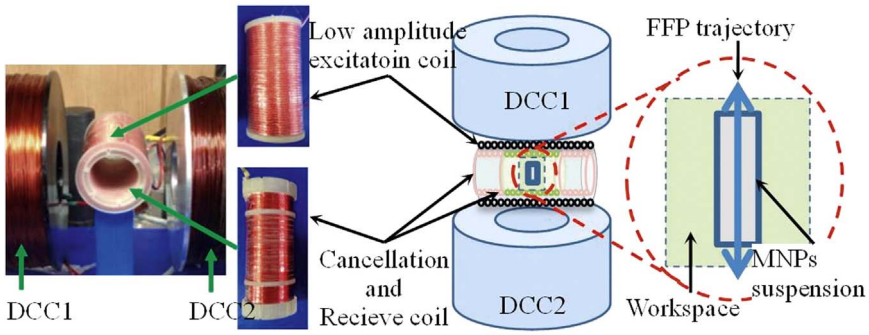

Fig. 4. The 1D nanoparticle navigation system used in the experiment (DCC: Differential-Current Coils, FFP: Field Fred Point).

$$mpi(t) = \begin{cases} 1 & NT_{hyb} < t \le NT_{hyb} + T_{mpi} \\ 0 & other\ \ value \end{cases}$$
$$ema(t) = \begin{cases} 1 & NT_{hyb} + T_{mpi} + T_{rel} < t \le (N+1)T_{hyb} - T_{rel} \\ 0 & other\ \ value \end{cases} \quad (7)$$

The differential currents $I_{DCC1,2}$ for MPI mode can be defined as follows;

$$I_{DCC1} = I^{DC} + I^{AC}\cos(2\pi f^{AC} t)$$
$$I_{DCC2} = I^{DC} - I^{AC}\cos(2\pi f^{AC} t) \quad (8)$$

where I^{DC} is the direct current offset, I^{AC} is the amplitude of alternating current (AC) component, and f^{AC} is the frequency of AC component. These sequences can select a mode for the navigation system of nanoparticles in each cycle as shown in Fig. 6. The developed navigation software coordinates four tasks; the actuation task which lasts 0.1 s, the relaxation task which lasts 0.05 s, the imaging acquisition task which lasts 0.3 s, and the reconstruction and control task, which is responsible for the MPI signal processing, image reconstruction, and controller routine. During the imaging task, a 0.7 A AC current (I^{AC}) was used to create and control the FFP. A 2 A direct current (I^{DC}) was used to offset each DCC, leading to a 4 cm FFP scanning range. The FFP scanning frequency of 0.1 s was determined

by the frequency of the AC current component, which was 5 Hz. The magnetic field gradient used to steer the nanoparticles was generated by a 5 A DCC. The field gradient was 3.5 T/m during the imaging and 8.75 T/m during the actuation.

The proposed hybrid system was designed and modeled in COMSOL Multiphysics software. Magnetic field results and trajectory analysis of nanoparticles for our actuation system have been discussed in detail in [13,16]. The currents of electromagnetic actuation (EMA), MPI and relaxation periods in left and right DCCs are shown in Fig. 7(a) and (b), respectively. The simulation results for trajectories of 90 nm-particles through the actuation are shown in Fig. 7(c). Nanoparticles move during both the imaging period and the actuation period. Since nanoparticles are exhibiting reciprocating movements in a small range, the force during imaging cycle does not affect significantly the displacements of the magnetic nanoparticles.

3. Experiment conditions

For coils configurations for the proposed 1D navigation system are shown in Fig. 4 and their specifications are shown in Table 1. The nanoparticle samples used to verify the 1D guidance system were 90 nm in diameter with a core size of 60–70 nm (MF-COO-0090, MagQu Co., Ltd.) and 45–65 nm diameter with a 5–6 nm core size (Resovist, Meito Sangyo Co., Ltd.) particles. The content of iron is used to describe content of SPIO in these two types of nanoparticles, and also estimate detection limit in MPI [17].

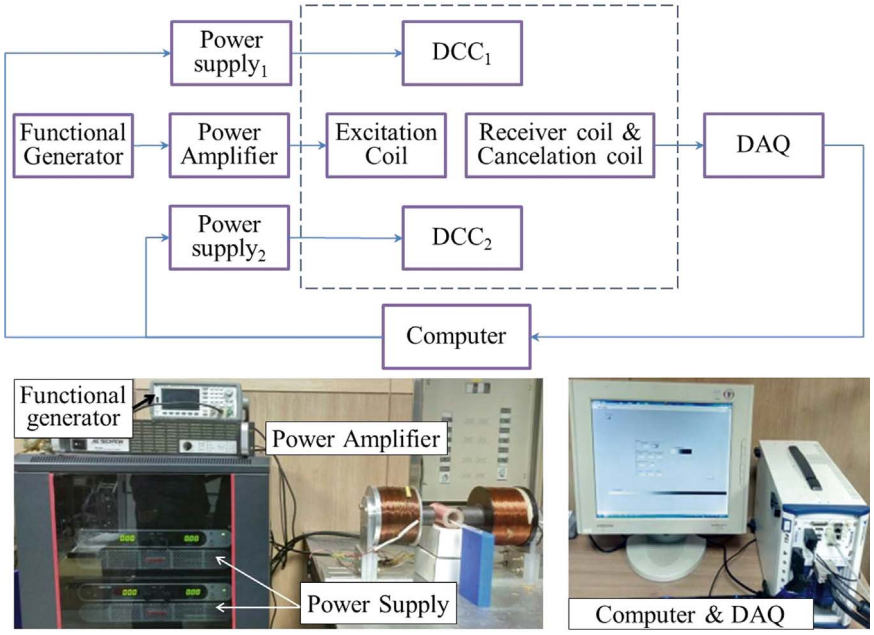

Fig. 5. Two power supplies, which are controlled separately by PC LabVIEW Controller, supply currents to differential-current coils (DCC) for generating field free point, moving field free point and generating gradient field to control magnetic nanoparticles. A current generated by a functional generator and amplified by a power amplifier is supplied to an excitation coil with low amplitude and high frequency. DAQ system is used to collect signals from a receive coil and a cancelation coil.

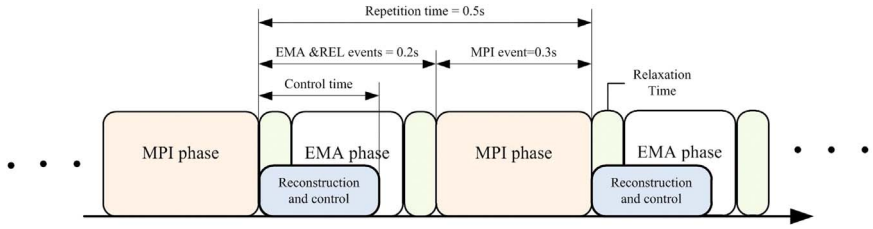

Fig. 6. The real-time navigation sequence of the magnetic nanoparticles. The navigation system generates FFP and moves FFP to cover interesting volume in MPI task; the original nanoparticles signal is also collected. The signals are reconstructed into images.

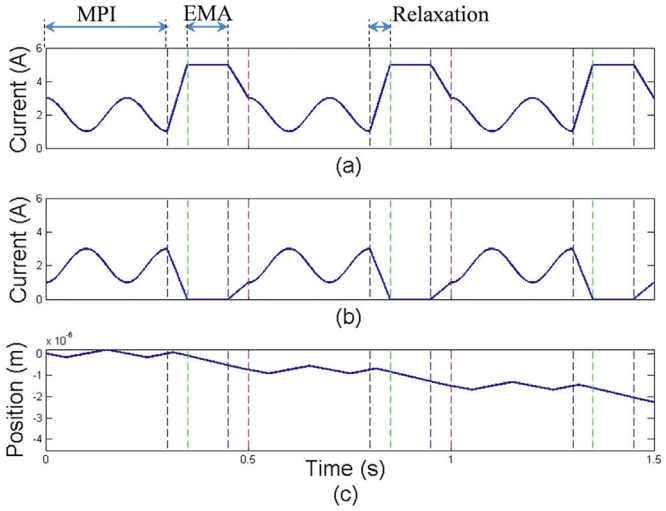

Fig. 7. Currents supply to DCCs in three hybrid periods. (a) and (b) are currents load in left DCC and right DCC respectively. (c) shows trajectory of single magnetic nanoparticle(core size: 60 nm) (EMA: electromagnetic actuation).

Table 1
Specification of coils.

	Turns	Inner diameter	Outer diameter	Coil length	wire
DCC	5000 each	7 cm	19 cm	7 cm	1 mm copper wire
Receive coil	400	4.2 cm	Single layer	6 cm	Litz wire
Cancelation coil	200 each	4.2 cm	Single layer	1.5 cm	Litz wire
Excitation coil	44	5 cm	Single layer	11 cm	Litz wire

For both samples, the suspension was diluted to 6.67 mg/mL-Fe and poured into a glass test tube with a 4.5 mm diameter. The length of the sample suspension inside the tube was about 20 mm, as shown in Fig. 8. The particles were able to move freely inside the glass tube. An oscillating 200μT field with a frequency of 40 kHz induced an output voltage of 1.53965 V when the system was empty and no selection field was applied. When a 100uL MagQu sample (6.67 mg/mL-Fe) was present, the output voltage was 1.54262 V. Hence, the nanoparticles induced a 2.97 mV change in amplitude. Therefore, output sensitivity of our navigation system is 224.6 μg/mV in amplitude. Based on this result, the unsaturated iron content in a neighborhood of the FFP, C_{Fe}, can be calculated. These signals were received by a device that was connected in series to the receiver coil and combined with the cancellation coil. To obtain the concentration of nanoparticles, the volume of the unsaturated suspension, V_{unsat}, and the number of particle per unit mass of iron, N_p, should be known. These two parameters that depend on magnetic field gradient, the magnetization characteristics, and the size distribution of particle are constant values

Fig. 8. Magnetic nanoparticle samples used in experiment, on the left is a MagQu nanoparticle, and on the right is a Resovist nanoparticle.

for particular kinds of nanoparticles. The nanoparticles concentration c_p can be expressed as:

$$c_p = c_{fe} N_p / V_{unsat} \quad (9)$$

Therefore, the nanoparticle concentration can be converted into the iron content with respect to particular nanoparticles.

4. Results and discussion

The nanoparticle samples were placed along the FFP scanning trajectory so that the distribution of their concentration could be monitored using MPI. Due to the electromagnetic actuation, the nanoparticles could move freely along the tube. The spatial resolution of the MPI determined the precision with which we could control our guidance system. The concentration of nanoparticles is estimated from the amplitude of received signal that is coupled with the excitation field, thus the resolution can be thought of as the largest distance between two adjacent peeks of received signal on the FFP trajectory. The resolution of our system is 0.014 mm. The positions of the maximum values in the MPI image were considered to indicate the center of nanoparticle cluster. In the experiment, the cluster was initially at the left end of the tube. We stopped guiding the particles when the cluster reached the right end of the tube. When using the MagQu nanoparticles, we monitored the position of the cluster using MPI and an optical camera. The results from experiments using both MagQu and Resovist nanoparticles are shown in Figs. 9 and 11, respectively. The grayscale images are reconstructed for MPI images, which show the concentration of the nanoparticles. Pure black color indicates a nanoparticle concentration of zero and pure white color

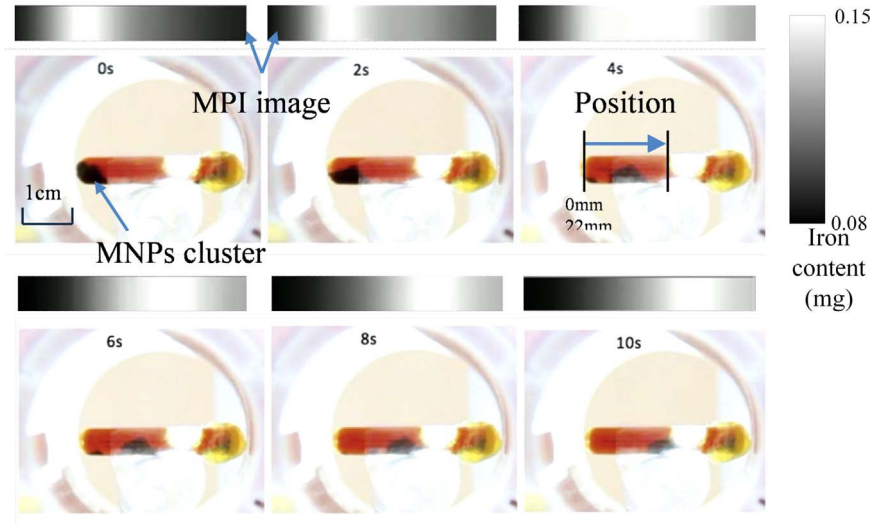

Fig. 9. The results from the experiments using the MagQu nanoparticles, which were manipulated by the navigation system. The magnetic force was in the right-hand direction. MPI (grayscale images) and camera images show the position of the particle cluster. The white regions indicate a higher nanoparticle concentration. During the actuation periods the force was towards the right. The legend shows the values of iron content at different positions, which indicates the magnetic nanoparticle distribution.

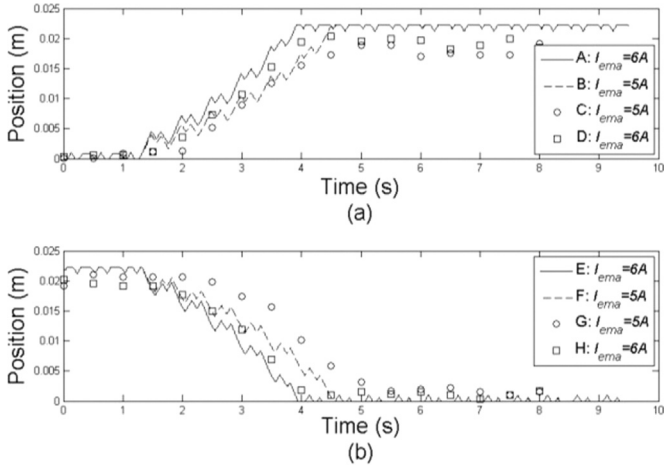

Fig. 10. Nanoparticles cluster positions reconstructed by the low-amplitude-excitation-field MPI and simulation trajectories under different currents during actuation (I_{ema}). (a) and (b) shows that the cluster was steered to the right and left. Curve A, B, E and F are simulation trajectories, while the data points C, D, G and H are the positions of the clusters' center from the real MPI image.

indicates the highest concentration of nanoparticles in the suspension. When a magnetic field was applied, the MagQu nanoparticles aggregated in a small cluster. The maximum values in the MPI image are thought to indicate the center of the cluster of nanoparticles. The cluster positions of experimental and simulation results during the navigation processing are shown in Fig. 10. In this experiment, the initial positions of cluster is in left end (0 mm) of tube, we set a constant current in the right coil and zero in the left coil to guide the cluster to move toward the right end of the suspension (22 mm) when the navigation system works in actuation mode. Imaging mode is monitoring the cluster displacements during the whole guidance process. The simulation results are also compared in Fig. 10(a). The positions of the max values from MPI image are seen as center of the nanoparticles cluster. The experimental results shown in Fig. 10 are mark as □ and ○. The nanoparticles cluster in simulation is assumed to be a 3 mm-diameter-sphere which is a combination of 10^9 nanoparticles. The results to the opposite direction guidance are shown in Fig. 10(b). This result shows that nanoparticles cluster positions reconstructed by the low-amplitude-excitation-field MPI are quite matching to the simulation trajectories under different currents during actuation.

For the dispersed Resovist nanoparticles, the navigation system has ability to control and monitor the Resovist nanoparticle concentration distribution. Due to the small core size, the Resovist nanoparticle hardly aggregated into a nanoparticle cluster under magnetic field in short time. When using the fresh water to dilute nanoparticle suspension, the distribution of concentration can be observed by a camera under high intensity light. The high concentration of nanoparticles will block the light passing through that is shown as low transmittance; on the contrary, the high transmittance indicates the low concentration. Fig. 11 shows some frames during the guidance process, under the right-directional magnetic force, the nanoparticles moved to the right side. The experiments shows the navigation system can monitor the positions of both nanoparticles cluster or the high concentration region of nanoparticles suspension (the lightest place in MPI image) and feed the information of the concentration back to the actuation periods, then, the system will guide nanoparticles to expected locations. Our 1D nanoparticle navigation system had a 2 Hz system refresh frequency (repetition frequency), which means that every 0.5 s the MPI image frame and control field were updated. This is an appropriate frequency for navigating capillaries in the brain and muscles, where the velocity of blood is approximately 1 mm/s [18].

To extend this 1D experimental system to a 3D navigation system, another two directional sets of coils, which induce fields orthogonal to each other, are arranged as shown in Fig. 3. These coils can act as the actuation coils in the actuation mode to steer nanoparticles in a 3D target region and the drive coils in the imaging period to monitor the nanoparticles distribution. By appropriate frequencies of currents chosen in these two sets of coils, a 3D Lissajous trajectory can be achieved to cover the 3D workspace, the received signal then can be reconstructed to 3D MPI images.

We estimated that if we adopted 24 Hz and 20 Hz sinusoidal currents in these two sets of coils during the MPI periods, the navigation system would remain in a 2 Hz system refresh frequency, which is possible for our current power supply (Sorensen SGA 17/600) with the voltage slew rate of 153 A/s.

For applications where the blood flows faster, a higher refresh frequency would be required. Increasing the actuation period would make the guidance system more effective, but would reduce the refresh frequency, resulting in fewer MPI images and lower feedback rate for the actuation. This would reduce the precision with which we could control the system. A longer MPI acquisition time would improve the MPI quality but reduce the actuation and control rates. The refresh

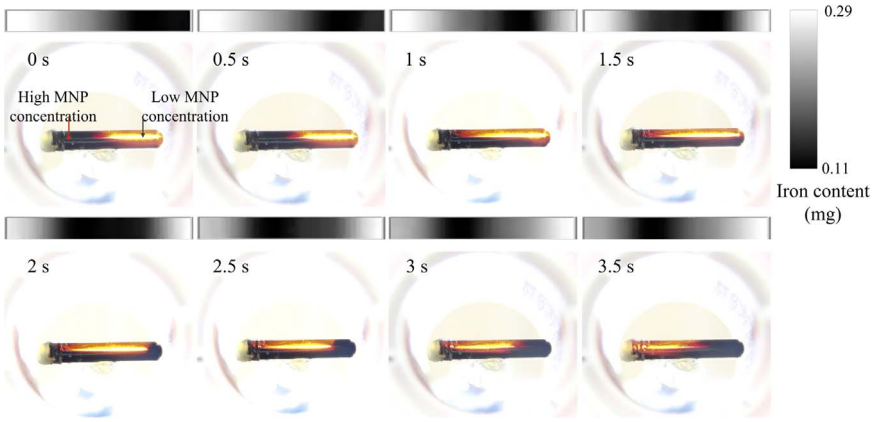

Fig. 11. The MPI and the camera images obtained when Resovist nanoparticles were used. The higher transmittance range of the samples indicates the lower nanoparticle concentration and the lower transmittance shows higher concentration. Again, the force was applied to the right during the actuation periods.

frequency can be increased as the nanoparticles can still be tracked if the MPI image quality is degraded.

5. Conclusion

Magnetic nanoparticles are becoming a promising choice as carrier particles in drug delivery systems for human body. The proposed navigation system for real-time actuation and monitoring of the nanoparticles will be inevitable for more precise targeting and diagnosis with spatial information of nanoparticles. It can be also cost efficient, compact, and optimized for precise targeting of the nanoparticles. The current design is suitable for a mouse brain, but it is not directly scalable to human brain. The results of our experiments and the methods described in this paper provide valuable data for the potential future enhancement of minimally invasive surgeries, intervention systems and procedures. Our new techniques can be adapted to a variety of applications, particularly the direct delivery of nanomedicine.

The current development is suitable for a mouse brain size workspace. The future work will focus on 3D system extension and scaling up to human brain size workspace. The low-amplitude-excitation-field MPI with the advantage of very low amplitude for high frequency excitation field is more feasible to enlarge field of view size. The disproportional scaling of magnetic fields and drag forces over human-sized workspaces, require higher gradient fields and magnetic field strengths. For *in vivo* imaging at human scale, several design improvements and innovations must be introduced to the present system. Real-time implementation of a mouse-sized system and experiments in a vascular network with many bifurcations will be the next another future works.

Acknowledgements

This research was supported by the Pioneer Research Center Program through the National Research Foundation of Korea funded by the Ministry of Science, ICT and Future Planning (2012-0009524) and in part by 2014R1A2A1A11053989.

References

[1] S.C. Mcbain, H.H. Yiu, J. Dobson, Magnetic nanoparticles for gene and drug delivery, Int. J. Nanomed. 3 (2) (2008) 169–180.
[2] B. Gleich, J. Weizenecker, Tomographic imaging using the nonlinear response of magnetic particles, Nature 435 (7046) (2005) 1214–1217.
[3] A.S. Lübbe, C. Bergemann, H. Riess, F. Schriever, P. Reichardt, K. Possinger, et al., Clinical experiences with magnetic drug targeting: a phase i study with 4′-epidoxorubicin in 14 patients with advanced solid tumors, Cancer Res. 56 (20) (1996) 4686–4693.
[4] T.D. Do, F.U. Amin, Y. Noh, M.O. Kim, J. Yoon, Guidance of magnetic nanocontainers for treating alzheimer's disease using an electromagnetic, targeted drug-delivery actuator, J. Biomed. Nanotechnol. 12 (3) (2016) 569–574.
[5] I.S.M. Khalil, L. Abelmann, S. Misra, Magnetic-based motion control of paramagnetic microparticles with disturbance compensation, IEEE Trans. Magn. 50 (10) (2014) 1–10.
[6] I.S.M. Khalil, P. Ferreira, R. Eleuterio, C.L. De Korte, S. Misra. Magnetic-based closed-loop control of paramagnetic microparticles using ultrasound feedback. Robotics and Automation (ICRA), 2014 IEEE International Conference on, 2014, pp. 3807-3812. IEEE
[7] S. Martel, J.B. Mathieu, O. Felfoul, A. Chanu, E. Aboussouan, S. Tamaz, et al., Automatic navigation of an untethered device in the artery of a living animal using a conventional clinical magnetic resonance imaging system, Appl. Phys. Lett. 90 (11) (2007) 114105.
[8] J.B. Mathieu, S. Martel, Steering of aggregating magnetic microparticles using propulsion gradients coils in an MRI scanner, Magn. Reson. Med. 63 (5) (2010) 1336–1345.
[9] B. Shapiro, S. Kulkarni, A. Nacev, S. Muro, P.Y. Stepanov, I.N. Weinberg, Open challenges in magnetic drug targeting, Wiley Interdiscip. Rev. Nanomed. Nanobiotechnology 7 (3) (2014) 446–457.
[10] E.U. Saritas, P.W. Goodwill, L.R. Croft, J.J. Konkle, K. Lu, B. Zheng, et al., Magnetic particle imaging (mpi) for nmr and MRI researchers, J. Magn. Reson. 229 (2) (2013) 116–126.
[11] C. Heyn, C.V. Bowen, B.K. Rutt, P.J. Foster, Detection threshold of single spio-labeled cells with fiesta, Magn. Reson. Med. Off. J. Soc. Magn. Reson. Med. 53 (2) (2005) 312–320.
[12] I.N. Weinberg, P.Y. Stepanov, S.T. Fricke, R. Probst, M. Urdaneta, D. Warnow, et al., Increasing the oscillation frequency of strong magnetic fields above 101 khz significantly raises peripheral nerve excitation thresholds, Med. Phys. 39 (5) (2012) 2578–2583.
[13] M.D. Tehrani, M.O. Kim, J. Yoon, A novel electromagnetic actuation system for magnetic nanoparticle guidance in blood vessels, IEEE Trans. Magn. 50 (2) (2014) 1–12.
[14] V. Schulz, M. Straub, M. Mahlke, S. Hubertus, A field cancellation signal extraction method for magnetic particle imaging, IEEE Trans. Magn. 51 (2) (2015) 1–4.
[15] P.W. Goodwill, S.M. Conolly, The x-space formulation of the magnetic particle imaging process: 1-d signal, resolution, bandwidth, snr, sar, and magnetostimulation, IEEE Trans. Med. Imaging 29 (11) (2010) 1851–1859.
[16] A. Mahmood, M. Dadkhah, M.O. Kim, J. Yoon, A novel design of an mpi-based guidance system for simultaneous actuation and monitoring of magnetic nanoparticles, IEEE Trans. Magn. 51 (2) (2015) 1–5.
[17] T. Knopp, T.M. Buzug, Magnetic particle imaging: an introduction to imaging principles and scanner instrumentation, Springer, 2012.
[18] K.P. Ivanov, M.K. Kalinina, Y.I. Levkovich, Blood flow velocity in capillaries of brain and muscles and its physiological significance, Microvasc. Res. 22 (2) (1981) 143–155.